07,10

Modeling of fracture and acoustic emission in polycrystalline solids with the discrete elements method

© V.L. Hilarov, E.E. Damaskinskaya

Ioffe Institute,
St. Petersburg, Russia

E-mail: Vladimir.Hilarov@mail.ioffe.ru

Received February 21, 2022
Revised February 21, 2022
Accepted February 24, 2022

The discrete element method (DEM) is used to reveal the main features of the fracture in materials with different degree of heterogeneity. It is shown that this method adequately describes the main properties of materials in the fracture process such as brittle and ductile behavior, two-staged nature of fracture in heterogeneous materials, heterogeneity of the spatial distribution of local internal stresses depending on the degree of heterogeneity.

Keywords: discrete element method, fracture of heterogeneous materials, computer modelling.

DOI: 10.21883/PSS.2022.06.54369.295

1. Introduction

There is still a priority task for fracture of construction, building and natural materials due to man-made and natural catastrophes taking place. At the same time, it is important to understand that the fracture is not a critical event, which can be avoided by using strength margin materials or geometric sizes, which are admittedly capable of withstanding specified mechanical loads. On the contrary, fracture is a process developing in space and time [1], in which material parameters such as elastic moduli, local mechanical stresses and deformations, structural rearrangements and discontinuities can be substantially changed. This process can be accompanied by various kinds of radiation (acoustic and electron emission, mechanic luminescence), whose parameters may indicate or precurse various kinds of events in the fracture process.

By a definition, traditional continuum methods of calculation of the strength characteristics (for example, the finite element method) do not allow explicitly taking into account material fracture (discontinuity). Instead of it, one considers a certain effective medium, in which the fracture is modelled by a specified phenomenological equation of state (usually, a nonlinear one), including a material fracture criterion. In contrast to these methods, the discrete element method (DEM) used in this study allows explicitly taking into account local discontinuities in the fracture process.

The present study has used a model of spherical particles (modeling the polycrystalline grains), which are interconnected by bonds (modeling the grain boundaries) in places of particle contacts. This model (bonded particle model — BPM) is described in detail in the paper [2], and its various modifications are widely used to study behavior of materials in mechanical fracture (for example, [3–8]). The BPM defines cracking nucleation as bond breaking between particles and their propagation — as merging of a multitude of broken bonds [9].

The purpose of the present paper was to study impact of the heterogeneity degree of the materials on a fracture nature and acoustic emission accompanying the fracture process. An elementary act of the acoustic emission was considered to be breaking of a single bond. The calculations were carried out in the freely distributable MUSEN software package [10].

2. Description of the numerical experiment

Cylindrical samples of the diameter 10 and height 20 mm have been modelled. They were sized to enable comparison of modeling results with laboratory results, which had been obtained earlier on the equally-sized samples. The cylinders were filled with spherical particles of same or different sized and packed by the MUSEM packing generator until obtaining the porosity 0.35−0.37. At the same time, overlapping of contacting spheres did not exceed 0.0001 mm.

For materials, from which the spherical grains and bonds therebetween (grain boundaries) are made of, materials with parameters of Table 1 were used. These parameters were specified as typical for rocks. It should be noted that „microscopic“ values of parameters for the particles and bonds differ from real values of the material parameters as a whole. That is why calibration of the „microscopic“ parameters is required to compare values of the mechanical properties of the modeling materials with the real ones [2,11]. As this paper has not tasked to compare numerical values of the magnitudes for the modeling and real materials (for example, a strength thereof), such parameter calibration was not carried out.

Table 1. Material parameters used in the modeling

№	Material	ρ, kg/m^3	E, GPa	ν	σ_n, MPa	σ_t, MPa	η, Pa · s
1	Granite	2700	45	0.13	175	175	5E19
2	Quartz	2650	94	0.29	600	600	5E19
3	Orthoclase	2560	62	0.29	420	420	1E19
4	Oligoclase	2560	70	0.29	480	480	1E19
5	Glass	2500	50	0.22	50	50	1E40
6	Quartz-orthoclase bond	2500	5.8	0.2	200	200	5E19
7	Quartz-oligoclase bond	2500	5.8	0.2	300	300	5E19
8	Orthoclase-oligoclase bond	2500	5.8	0.2	100	100	5E19

Note. Here: ρ — the material density, E — the Young modulus, ν — the Poisson ratio, σ_n — the material tensile strength, σ_t — the material shear strength, η — the dynamic viscosity.

Table 2. Grain diameters (mm) and percentage composition of each of the fractions

	Grain diameter of various fractions d_i, mm					Portion of each fraction, %
Quartz	0.36	0.188	0.52	0.28	0.42	0.0595745
Orthoclase	0.27	0.28	0.4	0.36	0.26	0.0702128
Oligoclase	0.16	0.168	0.288	0.24	0.4	0.0702128

Table 3. Grain diameters (mm) and percentage composition of each of the fractions

	Grain diameter of various fractions d_i, mm					Portion of each fraction, %
Quartz	0.09	0.047	0.132	0.079	0.106	0.0595745
Orthoclase	0.068	0.07	0.096	0.91	0.064	0.0702128
Oligoclase	0.041	0.042	0.077	0.063	0.098	0.0702128

Three sample types of the different heterogeneity degree were used:

1. Homogeneous sample of grains (particles) and bonds with granite properties (Table 1). The particle size is 0.4 mm, their number — 28125.

2. Grains (particles) with diameters and a percentage composition as specified in Table 2 (a particle diameter in millimeters, their number — 48695). The sizes were a set of values with the mean value of 0.3 mm and the standard deviation of 0.1 mm, which was obtained by means of a random number generator with normal distribution.

3. Grains (particles) with diameters and a percentage composition as specified in Table 3 (a particle diameter in millimeters, their number — 33670). The said sizes were a set of values with the average value of 0.08 mm and the standard deviation of 0.025 mm, which was obtained by means of a random number generator with normal distribution. The fraction diameter 4 for orthoclase is ten times increased in order to improve the heterogeneity degree.

The bonds were formed in places of particle contacts. The bond materials was selected from Table 1. The particles of the same material were connected with a bond of the same material, while the particles of the different materials were connected either by low-strength brittle glass bonds 5 (hereinafter — a set of bonds of the type 1), or low-module bonds 6, 7, 8 [12] (hereinafter — a set of bonds of the type 2). The bond diameter (d) was selected automatically by a bond generator to equal to a lesser diameter of a pair of the connected particles 1 and 2: $d = \min\{d_1, d_2\}$ [10]. The maximum bond length ($L_{\max}$) was selected to disable one more particle between the pair of the connected particles. The minimum length $L_{\min}$ was usually zero. It should be noted that this selection of $L_{\min}$ can have the system spontaneously blow up, as the above-mentioned particle overlapping was allowed. If it occurred, the minimum bond length was accepted to equal to the maximum overlapping (0.0001 mm) with a reverse sign.

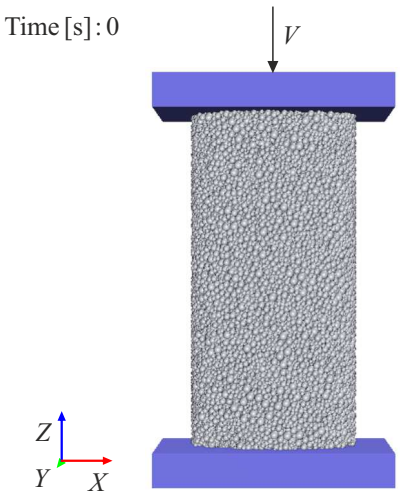

Figure 1. Sample and diagram of the modeling experiment.

Then, the sample was placed in a virtual press, whose lower plate was fixed, while its upper plate was moving to the lower one at the speed of $V = 0.02$ m/s until fracture of the sample (Fig. 1). The fracture process, in equal time periods — a data saving time interval — recorded a large set of data of various mechanical parameters of the sample, which could be used for further analysis.

3. Results and discussion

The Fig. 2 shows the loading diagrams of the samples of the different heterogeneity and the homogeneous sample. The deformation was calculated by the formula $\varepsilon = Vt$. The stresses were calculated based on forces acting on the loading plates. Since the numerical experiment usually makes it impossible to sustain an equality of forces acting on the plates [13], the stress was calculated by the formula $\sigma = 0.5(F_t + F_b)/S$, where the indices t and b signify the top and the bottom, S — the sample section (the section at the initial time moment was used).

It is seen that it is typical for more homogeneous samples (1 and 2 of Fig. 2, *a* and Fig. 2, *b*) to exhibit brittle behavior (linear increase of stress) and sharp drop of stresses after obtaining its maximum value. It is typical for more heterogeneous samples (the curves 3–5, Fig. 2, *a*) to exhibit a nonlinear (plastic) section on the loading diagram. It is due to the fact that first weaker bonds are broken, and so are stronger ones, then.

The model also allows studying the kinetics of bond breaking in time. The results are shown in the Fig. 3 and include the number of bonds broken during the data saving time interval (10^{-5} s for Fig. 3, *a* and 10^{-4} s for Fig. 3, *b* and 3, *c*) — of „the acoustical activity“ (AA).

The Fig. 3 clearly shows the difference in the behavior of „the acoustic activity“ for the homogeneous and heterogeneous materials. The former ones (Fig. 3, *a, b*) are characterized by a very small number of broken bonds up to the fracture, when there is a maximum value of the stresses of Fig. 2. There is an AA burst at this moment. The heterogeneous sample starts to accumulate bond breaks in the plastic region, when the weakest bonds start to break. Note that the mechanical properties of the materials modelled in the present paper are mostly affected by heterogeneity and mechanical properties of the grain boundaries (bonds), while the grain (particle) properties are not essential. It is due to the fact that in accordance with the model under study the particles themselves do not collapse.

The analysis of heterogeneity of bond breaking across the sample bulk is shown in the Fig. 4. The sample was divided into 10 layers along the height and fracture parameters were calculated in each layer for each saved moment of time. The Fig. 4, *a* shows the time dependence of the number of unbroken bonds averaged across the layers (N) for the three samples under study. A spatial heterogeneity measure was selected to be a variation coefficient of the number of

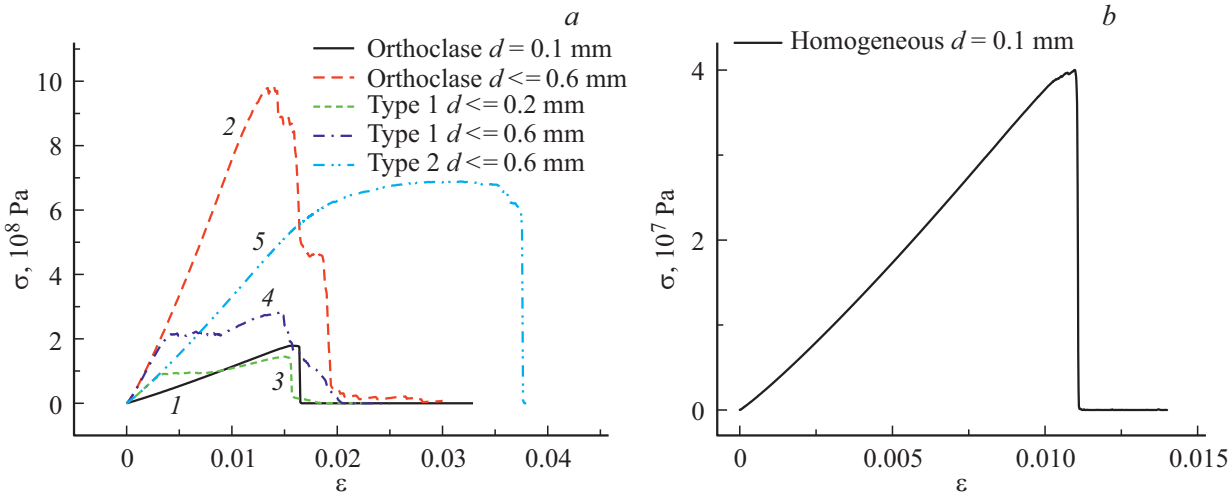

Figure 2. Diagrams of loading the samples with the different type of bonds (*a*) and the homogeneous sample (*b*).

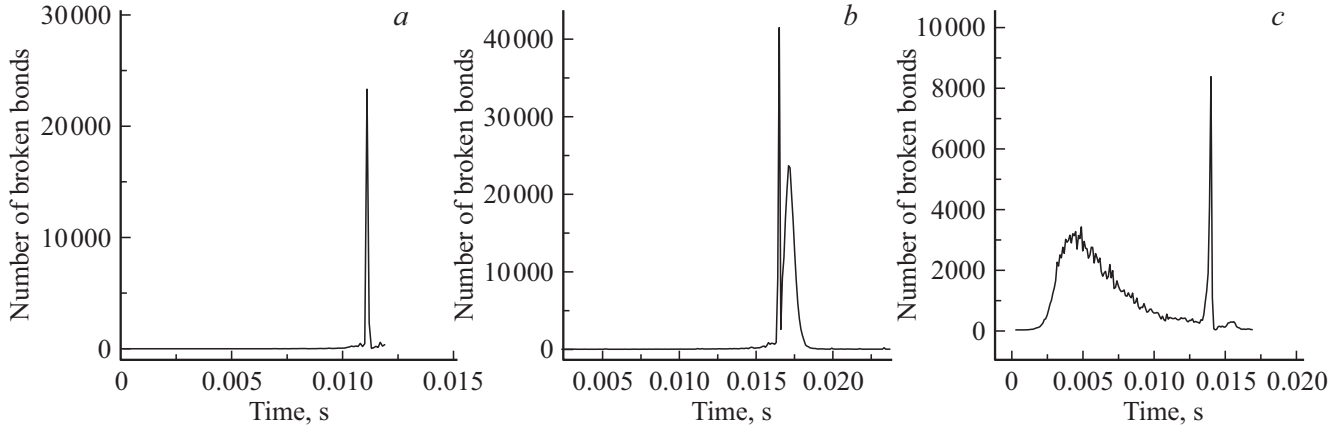

Figure 3. „Acoustical activity“ — the number of bonds broken per unit time in the homogeneous sample (*a*); the sample with one bond type (orthoclase) (*b*) and the sample with different bonds (of the type 1). Bond diameter $d = 0.1$ mm.

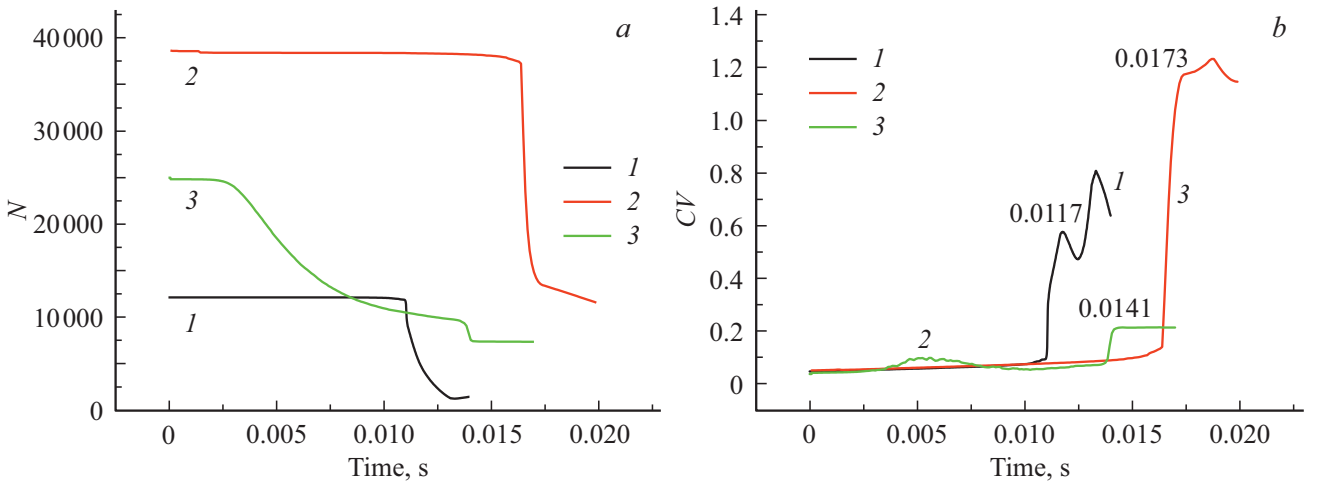

Figure 4. Time dependence of the number of unbroken bonds averaged across the layers (N) (*a*) and the variation coefficient (CV): *1* — the homogeneous sample, *2* — the sample with orthoclase bonds, *3* — the sample with bonds of the type 1 from Table 1.

unbroken bonds across the layers (CV). Its time dependence is shown in the Fig. 4, *b*.

The samples *1* and *2* have evident brittle fracture: an insignificant reduction of the number of unbroken bonds with a low variation coefficient (bulk homogeneity) during long modeling time and an explosion-like jump of CV near the sample fracture time (fracture localization and cracking growth). The heterogeneous sample *3* accumulates damage within significantly less periods of time. However, the variation coefficient at this stage is also small, which confirms that the damage is accumulated more or less homogeneously across the sample bulk. It confirms that a model of the two-stage fracture of heterogeneous materials proposed in the papers [14,15] is true. The variation coefficient jump is also not very high. It corresponds to a uniform fracture type in the heterogeneous samples found earlier in the laboratory experiments [16], and to a similar result obtained in a cellular automaton model [17].

Each layer has been calculated for maximum tension stresses on the bonds $\sigma_{\max}$. The Fig. 5, *a* shows the time dependences of the values $\langle\sigma_{\max}\rangle$ averaged across the layers. Causes of local tension stresses under the action of an external compression stress are well known (see, for example, [2]) and are not discussed here. These stresses are obtained by averaging the maximum stresses across the layers in each layer at each saved moment of time. The Fig. 5, *b* shows the time dependences of the variation coefficient of the magnitude $\sigma_{\max}$ across the layers.

In order to understand the time behavior of the tension stresses, it should be kept in mind that a structure of grains and their boundaries (particles and bonds) created at the material formation stage is not an equilibrium one and has significant internal local stresses. The initial stage of mechanical loading includes relaxation of these stresses. It is manifested in nonmonotonicity of their time dependence at this stage (Fig. 5, *a*) and a significant variation coefficient in the Fig. 5, *b*. With relaxation of the stresses, they are

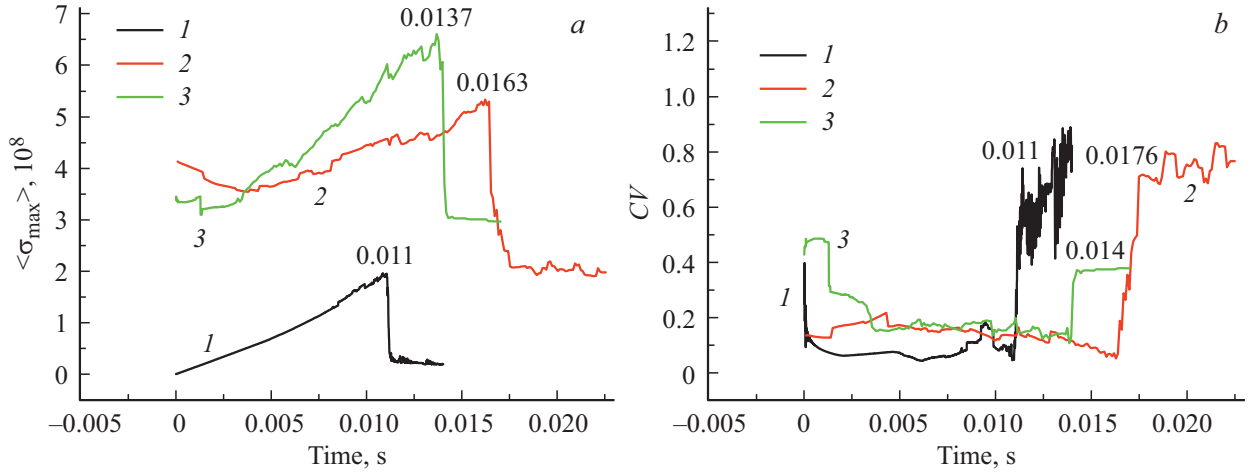

Figure 5. Maximum tension stresses averaged across the layers (*a*) and their variation coefficients (*b*): *1* — the homogeneous sample, *2* — the sample with orthoclase bonds, *3* — the sample with bonds of the type 1 from Table 1.

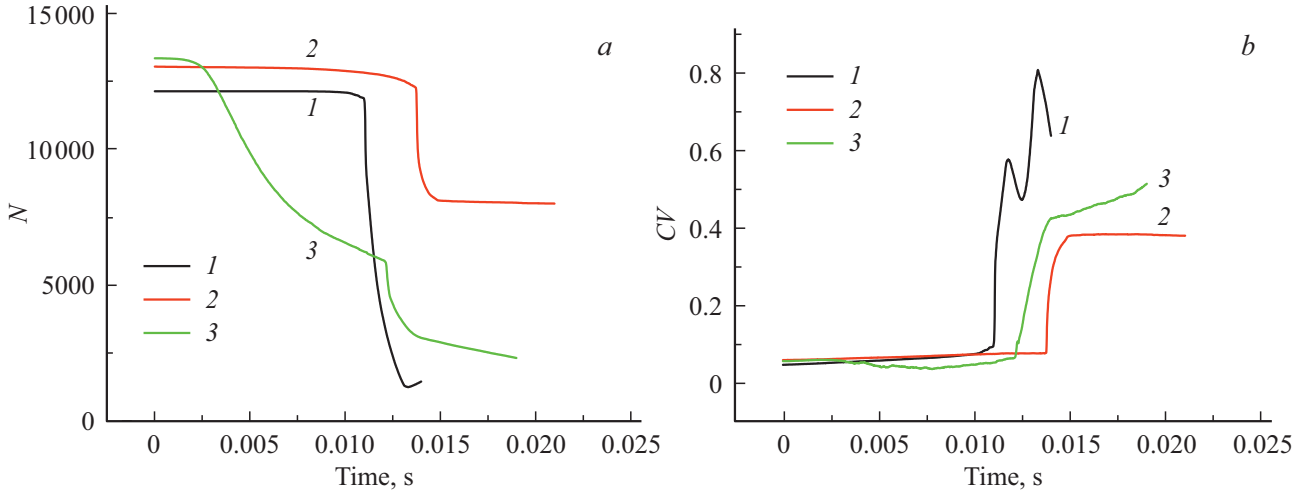

Figure 6. Bond breaking kinetics and its variation coefficient for the samples with particle parameters from Table 3. *1* — the homogeneous sample, *2* — the sample with orthoclase bonds, *3* — the sample with bonds of the type 1 from Table 1.

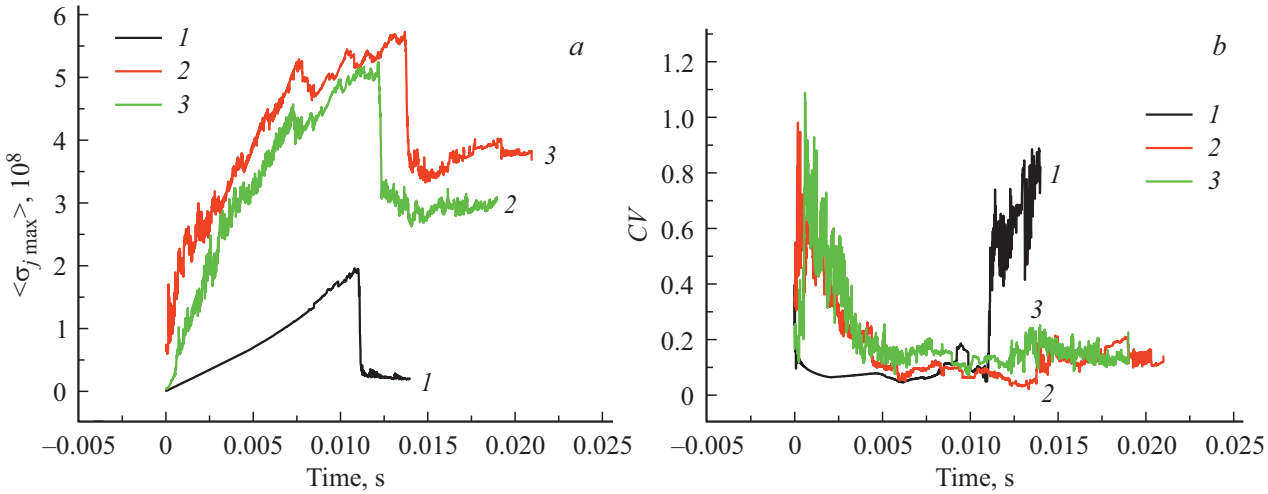

Figure 7. Maximum tension stresses and their variation coefficients for the samples with the particle parameters from Table 3. *1* — the homogeneous sample, *2* — the sample with orthoclase bonds, *3* — the sample with bonds of the type 1 from Table 1.

levelled across the bulk (Fig. 5, *b*) and increased (Fig. 5, *a*) until setting up conditions for formation of a fracture focus. When the focus is formed, the local stresses become substantially heterogeneous across the bulk (Fig. 5, *b*) again, wherein a value of this heterogeneity in the heterogeneous sample is much less than in more homogeneous ones.

Impact of the heterogeneity of the grain size distribution was revealed by studying the samples, in which the grain size of one of the orthoclase fractions was increased in one order (0.91−0.091 mm) in comparison with its value, which had been obtained by means of the random number generator with normal distribution (Table 3). The other parameters were the same as for the samples discussed above. The homogeneous sample in the present and previous series is the same.

The Fig. 6 shows the bond breaking kinetics and its variation coefficient as in the Fig. 4, the Fig. 7 — the maximum stresses and their variation coefficients as in the Fig. 5.

It is clear that the results for the bond breaking kinetics in this series (Fig. 6) are similar to those as in the Fig. 4. The increased heterogeneity of the particle size distribution led to the significantly reduced variation coefficient for the sample with orthoclase bonds at the last (focus) fracture stage. The same happened for the variation coefficient of local stresses for this sample. Thus, the additionally increased heterogeneity of the sample led to the increased homogeneity degree of its fracture nature, i.e. a multi-focus type.

4. Conclusion

It seems that the discussed model of polycrystalline materials realistically describes some features of their fracture when the main processes proceed along the grain boundaries. These features include a brittle fracture nature of the homogeneous materials and a nonlinear elasticity (plasticity) for more heterogeneous materials, which were revealed by means of the loading diagram sigma−epsilon (the equation of state) and the time behavior of „the acoustic activity“ — the number of broken bonds per unit time. For the heterogeneous materials, the model predicts the two-staged type of their fracture, i.e. the first stage includes accumulation of flaws homogeneously across the sample, while the second stage — formation and growth of the fracture focus.

The calculation of the maximum local stresses showed that the material homogeneity leads to the higher heterogeneity of the local stresses in space and, vice versa, the heterogeneity contributes to their higher homogeneity. The same behavior of the local internal stresses, which are calculated based on the S.N. Zhurkov kinetics concept, was noted in laboratory experiments in the paper [16].

We assume that further computer experiments and their analysis will allow comparing the size distribution of defects evolving in time during fracture and the energy distribution of the acoustic emission signals. It will allow finding out what conditions a transition from the Markov process to a state of the self-organized criticality.

Conflict of interest

The authors declare that they have no conflict of interest.

References

[1] S.N. Zhurkov. J. Fracture Mech. **1**, 311 (1965).
[2] D.O. Potyondy, P.A. Cundall. Int. J. Rock Mech. Min. Sci. **41**, 1329 (2004).
[3] J.F. Hazzard, R.P. Young. Int. J. Rock Mech. Min. Sci. **37**, 867 (2000).
[4] H. Hofmann, T. Babadagli, G. Zimmermann. Int. J. Rock Mech. Min. Sci. **77**, 152 (2015).
[5] Harsh B. Vora, Julia K. Morgan. J. Geophys. Res.: Solid Earth. **124**, 7993 (2019).
[6] N. Cho, C.D. Martin, D.C. Sego. Int. J. Rock Mech. Min. Sci. **44**, *7*, 997 (2007).
[7] J.F. Hazzard, R.P. Young. Tectonophys. **356**, *1−3*, 181 (2002).
[8] X.P. Zhang, L.N.Y. Wong. Rock Mech. Rock Eng. **45**, *5*, 711 (2012).
[9] A. Lisjak, G. Grasselli. J. Rock Mech. Geotech. Eng. **6**, 301 (2014).
[10] M. Dosta, V. Skorych. Software **X12**, 100618 (2020).
[11] T. Kazerani, J. Zhao. Int. J. Numer. Anal. Meth. Geomech. **34**, *18*, 1877 (2010).
[12] X.F. Li, Q.B. Zhang, H.B. Li, J. Zhao. Rock Mech. Rock Eng. **51**, 3785 (2018).
[13] N.J. Brown. Discrete Element Modelling of Cementitious Materials. Ph.D. Thesis. The University of Edinburgh (2013). 247 p.
[14] S.N. Zhurkov, V.S. Kuksenko. Mekhanika polimerov **10**, *5*, 792 (1974) (in Russian).
[15] V. Kuksenko, N. Tomilin, E. Damaskinskaya, D. Lockner. Pure Appl. Geophys. **146**, 253 (1996).
[16] V.L. Hilarov, E.E. Damaskinskaya. Physics of the Solid State **63**, *6*, 783 (2021).
[17] V.L. Hilarov. Physics of the Solid State **53**, *4*, 707 (2011).